

Adversarial Ensemble Training by Jointly Learning Label Dependencies and Member Models

Lele Wang, [†]Bin Liu

Abstract—Training an ensemble of different sub-models has empirically proven to be an effective strategy to improve deep neural networks’ adversarial robustness. Current ensemble training methods for image recognition usually encode the image labels by one-hot vectors, which neglect dependency relationships between the labels. Here we propose a novel adversarial training approach that learns the conditional dependencies between labels and the model ensemble jointly. We test our approach on widely used datasets MNIST, FashionMNIST and CIFAR-10. Results show that our approach is more robust against black-box attacks compared with state-of-the-art methods. Our code is available at <https://github.com/ZJLAB-AMMI/LSD>.

Index Terms—adversarial training, ensemble, deep neural networks, label dependency

I. INTRODUCTION

Learning with deep neural networks (DNNs), also known as deep learning, has achieved astonishing successes for many tasks in computer vision [1]–[4], speech recognition [5], [6], and natural language processing [7], [8]. However, many works show that modern DNNs are vulnerable to adversarial attacks [9]–[14]. In particular, even a slight perturbation to an input image that is imperceptible to humans may fool a high-performing deep neural network (DNN) to produce a wrong prediction. Moreover, adversarial attacks generated for one model may mislead other models to yield wrong predictions, which is an issue called adversarial transferability [15]–[18]. Such adversarial vulnerability issues pose a grand challenge for real-life applications of DNNs, especially for safety-critical problems such as self-driving cars [19], [20]. The study on promoting robustness against adversarial attacks for DNNs has attracted more and more attentions.

Model ensemble has shown to be an effective strategy to improve the adversarial robustness of a deep learning system. The basic idea of model ensemble can be depicted via a Venn diagram as shown in Fig. 1 [21]. The region enclosed by the rectangle represents the space spanned by all possible orthogonal perturbations to the input, the sub-region enclosed by a circle represents the subspace spanned by perturbations that are adversarial to the associated model, and the shaded region represents the perturbation subspace that is adversarial to the model ensemble. For a single model case corresponding to Fig.1(a), any perturbation within the subspace marked by the circle causes the model to misclassify the input. In contrast, for cases that employ an ensemble of two models, corresponding to Fig.1(b) and (c), only perturbations within the subspace marked by the shaded region lead to a successful

adversarial attack. In another word, the adversarial input has to fool all models in the ensemble to produce a successful adversarial attack. Indicated by Fig.1(b) and (c), we see that an intuitive strategy to improve the adversarial robustness of a model ensemble is to promote the diversity of the individual models, as the more diversified among the individuals, the less overlapped among their corresponding adversarial subspaces. The amount of overlap determines the dimensionality of the adversarial subspace [21]. In what follows, we use the terms individual model, sub-model, and member model interchangeably, and their meanings are the same.

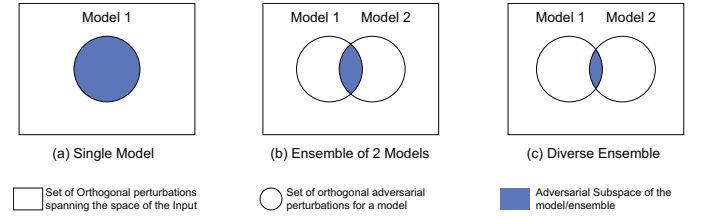


Fig. 1. A conceptual illustration of the idea of using model ensembling to promote adversarial robustness: (a) single model; (b) an ensemble of two models; (c) an ensemble of two more diversified models. The shaded region denotes a subspace, adversarial attacks within which can fool the (ensemble) model to make a wrong prediction.

A disturbing issue is how to promote the diversity of the member models in the ensemble while preserving their accuracy, especially for non-adversarial inputs. Simply put, the question is: how to balance the member models’ diversity and their qualities during the ensemble training process? To this end, several advanced ensemble training methods have been proposed in the literature [21]–[25]. For instance, Pang et al. propose a diversity regularized cost function to be minimized, which encourages diversity in the distributions of non-maximal predictions given by the models [22]. Kariyappa & Qureshi select to train an ensemble of gradient misaligned models by minimizing their pairwise gradient similarities [21]. Yang et al. find that only encouraging the misalignment between pairwise gradients is not enough to reduce adversarial transferability [25]. They propose to promote not only model orthogonality but also model smoothness. Sen et al. propose to train an ensemble of models with different numerical precisions, in which models with higher numerical precisions target the goal of prediction precision, while those with lower numerical precisions target that of adversarial robustness [23].

As aforementioned, usually an ensemble training method will select a diversity metric. It may be the difference in the distributions of non-maximal predictions of the member models [22], or the difference in the gradient vectors associated

Lele Wang and Bin Liu are with Zhejiang Lab, Hangzhou, China. Emails: {wangll, liubin}@zhejianglab.com. [†]Corresponding author.

with the member models [21]. A common feature of these ensemble training methods is that all of them select the one-hot vector to encode the image classes. That says every image is assigned with a hard label. Such hard labels can not reflect any possible dependency relationships between the image classes. Given an image, it is likely to find dependency relationships between the image classes. For example, in a handwritten digit image dataset, number “0” may look more similar to number “9” than to “4”; “3” may look more similar to number “8” than to “7”, and so on. Conditional on a noisy input image, e.g., one whose ground truth label is “0”, there should exist a dependency relationship between labels “0” and “9”. Using a hard labeling setting, one omits such conditional dependency relationships.

Motivated by the above observation, we propose a novel ensemble training algorithm, Conditional Label Dependency Learning (CLDL) assisted ensemble training, which learns the conditional dependencies between the image classes and the model ensemble together. Compared with the existent ensemble training methods, our method selects an different diversity metric, which measures both the difference in the pairwise gradient vectors associated with the member models and that between the predicted soft labels given by the member models. The soft labels encode the dependency relationships between the original hard labels. We find that our method is more robust against black-box attacks compared with some state-of-the-art (SOTA) methods.

To summarize, the main contributions of this work are:

- We propose a novel diversity metric for adversarial ensemble training. This metric covers information underlying both the gradient vectors associated with the member models and the predicted soft labels given by the member models.
- We adapt a label confusion learning (LCL) model developed in [26], which is originally used for enhancing text classification, to generate soft labels of images in the context of adversarial ensemble training.
- We propose a CLDL assisted ensemble training algorithm and demonstrate that it complements the existent ensemble training methods. In particular, we show that our algorithm is more robust against black-box attacks compared with several SOTA methods considered.
- We open-source our code at <https://github.com/ZJLAB-AMMI/LSD>.

The rest of this paper is organized as follows. In Section II, we present some preliminary information. In Section III, we describe our CLDL based ensemble training method in detail. In Section IV, we present the experimental results. We conclude the paper in Section V.

II. PRELIMINARY

In this section, we present the preliminary knowledge that is related to our work.

A. Notations

Here we consider a DNN based image recognition task, which involves C classes. Following [25], let \mathcal{X} denote the

input space of the DNN model, $\mathcal{Y} = \{1, 2, \dots, C\}$ the class space. A DNN model is trained to yield a mapping function $\mathcal{F} : \mathcal{X} \rightarrow \mathcal{Y}$. Let x denote a clean image and x' an adversarial counterpart of x . Let ϵ be a pre-set attack radius that defines the maximal magnitude of an adversarial perturbation. That says, for any adversarial perturbation, its L_p norm is required to be less than ϵ . Let $\ell_{\mathcal{F}}(x, y)$ denote the cost function used for training the model $\mathcal{F}(x, \theta)$, where θ denotes the parameter of the model.

B. Definitions

Definition 1. Adversarial attack [25]. Given an input $x \in \mathcal{X}$ with true label $y \in \mathcal{Y}$, $F(x) = y$. (1) An untargeted attack crafts $\mathcal{A}_U(x) = x + \delta$ to maximize $\ell_{\mathcal{F}}(x + \delta, y)$ where $\|\delta\|_p \leq \epsilon$. (2) A targeted attack with target label $y_t \in \mathcal{Y}$ crafts $\mathcal{A}_T(x) = x + \delta$ to minimize $\ell_{\mathcal{F}}(x + \delta, y_t)$ where $\|\delta\|_p \leq \epsilon$ and ϵ is a pre-defined attack radius that limits the power of the attacker.

Definition 2. Alignment of loss gradients [21], [25]. The alignment of loss gradients between two differentiable loss functions $\ell_{\mathcal{F}}$ and $\ell_{\mathcal{G}}$ is defined as:

$$CS(\nabla_x \ell_{\mathcal{F}}, \nabla_x \ell_{\mathcal{G}}) = \frac{\nabla_x \ell_{\mathcal{F}}(x, y) \cdot \nabla_x \ell_{\mathcal{G}}(x, y)}{\|\nabla_x \ell_{\mathcal{F}}(x, y)\|_2 \cdot \|\nabla_x \ell_{\mathcal{G}}(x, y)\|_2} \quad (1)$$

which is the cosine similarity between the gradients of the two loss functions for an input x drawn from \mathcal{X} with any label $y \in \mathcal{Y}$. If the cosine similarity of two gradients is -1, we say that they are completely misaligned.

Definition 3. Transferability [25]. Consider an adversarial instance $\mathcal{A}_U(x)$ or $\mathcal{A}_T(x)$ constructed against a surrogate model \mathcal{F} . With a given benign input $x \in \mathcal{X}$, the transferability T_r between \mathcal{F} and a target model \mathcal{G} is defined as follows:

$$\begin{aligned} \text{Untargeted:} \quad & T_r(\mathcal{F}, \mathcal{G}, x) \\ \mathbb{I}[\mathcal{F}(x) = \mathcal{G}(x) = y \wedge \mathcal{F}(\mathcal{A}_U(x)) \neq y \wedge \mathcal{G}(\mathcal{A}_U(x)) \neq y] &= \\ \text{Targeted:} \quad & T_r(\mathcal{F}, \mathcal{G}, x, y_t) \\ \mathbb{I}[\mathcal{F}(x) = \mathcal{G}(x) = y \wedge \mathcal{F}(\mathcal{A}_T(x)) = \mathcal{G}(\mathcal{A}_T(x)) = y_t] &= \end{aligned}$$

where $y_t \in \mathcal{Y}$ denotes the adversarial target. For untargeted attacks, attacking transferability happens if both the surrogate model and target model can make correct predictions for the benign inputs, but both of them make incorrect predictions for the adversarial input $\mathcal{A}_U(x)$, which is generated by untargeted attacks against the surrogate model \mathcal{F} . For targeted attacks, attacking transferability means that both the surrogate and the target models can make correct predictions for benign inputs, but both of them give a prediction result $y_t \in \mathcal{Y}$ for the adversarial input $\mathcal{A}_T(x)$, which is generated by targeted attacks against the surrogate model \mathcal{F} .

C. Adversarial Attacks

Adversarial attacks aim to generate human-imperceptible adversarial inputs that can fool a high-performing DNN to make wrong predictions. Usually they are divided into two basic classes, namely, white-box attack, which assumes that the adversary is fully aware of the model’s structures and parameters, and black-box attack, which assumes that the adversary has no access and is not aware of any information

about the model. Here we only introduce four typical white-box attacks briefly that are involved in our experiments, while refer readers to review papers [27]–[29] and references therein for more information on adversarial attacks.

Fast Gradient Sign Method (FGSM) FGSM is a typical white-box attacking method to find adversarial examples. It performs a one-step update along the direction of the gradient of the adversarial loss. Specifically, it generates an adversarial example x' by solving a maximization problem as follows [9]:

$$x' = x + \varepsilon \cdot \text{sign}(\nabla_x \ell(x, y)), \quad (2)$$

where ε denotes the magnitude of the perturbation, x the original benign image sample, y the target label of x , and $\nabla_x \ell(x, y)$ the gradient of the loss $\ell(x, y)$ with respect to x .

Basic Iterative Method (BIM) BIM is an extension of FGSM, which performs FGSM iteratively to generate an adversarial example as follows [30]:

$$x'_i = \text{clip}_{x, \varepsilon} \left(x'_{i-1} + \frac{\varepsilon}{r} \cdot \text{sign}(g_{i-1}) \right) \quad (3)$$

where $x'_0 \triangleq x$, r is the number of iterations, $\text{clip}_{x, \varepsilon}(A)$ is a clipping function that projects A in a ε -neighbourhood of x , and $g_i \triangleq \nabla_x \ell(x'_i, y)$.

Projected Gradient Descent (PGD) PGD [12] is almost the same as BIM, the only difference being that PGD initialize x'_0 as a random point in the ε -neighbourhood of x .

Momentum Iterative Method (MIM) MIM is an extension of BIM. It updates the gradient g_i with the momentum μ as follows [31]:

$$x'_i = \text{clip}_{x, \varepsilon} \left(x'_{i-1} + \frac{\varepsilon}{r} \cdot \text{sign}(g_i) \right) \quad (4)$$

where $g_i = \mu g_{i-1} + \frac{\nabla_x \ell(x'_{i-1}, y)}{\|\nabla_x \ell(x'_{i-1}, y)\|_1}$, and $\|\cdot\|_1$ denotes the L_1 norm.

Instead of focusing on the methods of attack, in this paper, we focus on training a robust model to achieve higher robustness and better classification performance.

D. On techniques to generate soft labels

Label smoothing is perhaps the most popularly used technique to generate soft labels [4], [32]–[34]. Despite of being simple, it has been demonstrated as an effective approach to improve the accuracy of deep learning predictions. Specifically, Szegedy et al. propose to generate soft labels by averaging the one-hot vector formed label distribution and a uniform distribution over labels [4]. Fu studies the effect of label smoothing on adversarial training and find that adversarial training with aid of label smoothing can enhance model robustness against gradient-based attacks [35]. Yida Wang proposes an Adaptive Label Smoothing approach that can adaptively estimate a target label distribution [36]. Guo et al. propose a label confusion model (LCM) to improve text classification performance [26], which is adapted here for CLDL and generating soft labels in the context of adversarial ensemble training.

III. THE PROPOSED CLDL ASSISTED ENSEMBLE TRAINING METHOD

We illustrate conceptually our model in Figure 2, which takes an ensemble of two models for example for ease of presentation. Our model is mainly composed of two parts: an ensemble of N sub-models ($\{\mathcal{F}_i(x, \theta_i)\}_{i \in [N]}$) ($N = 2$ in Figure 2) and a label confusion model (LCM).

Each sub-model in the ensemble consists of an input CNN encoder followed by a fully connected classifier, which can be any main stream deep learning based image classifier. As shown in Figure 2, an image (x) to be classified is fed into the input-encoder to generate an image representation (v_i), which is then fed into the fully connected classifier to predict the label distribution of this image:

$$\begin{aligned} v_i &= \mathcal{F}_i^{\text{encoder}}(x) \\ p_i &= \text{softmax}(Wv_i + b) \end{aligned} \quad (5)$$

where $\mathcal{F}_i^{\text{encoder}}(\cdot)$ is the outputs of input-encoder of \mathcal{F}_i , transforming the input x to the input image representation v_i with dimension d . p_i is the predicted label distribution (PLD).

The LCM consists of two parts, a label encoder and a simulated label distribution (SLD) computation block. The form of the label encoder is a DNN, which is used to generate the label representation matrix [26]. The SLD block is composed of a similarity layer and an SLD computation layer. The similarity layer takes the label representations and the current instance representation as inputs, and computes their similarity values by dot product, which are then fed into a soft-max activation layer, which outputs the label representation vector (LCV).

The LCV captures the conditional dependencies among the image classes by calculating the similarity between the instance representations and the label representations. The LCV is instance-dependent, which considers the similarity among labels conditional on a specific image instance. Following [26], the corresponding one-hot vector y_i is added to the LCV with a controlling parameter γ , which is then normalized by a soft-max function that generates the SLD. The controlling parameter γ decides how much of the one-hot vector will be changed by the LCV. The above process can be formulated by:

$$\begin{aligned} \text{Vec}^{(l)} &= f^L(l) = f^L([l_1, l_2, \dots, l_C]) = [\text{Vec}_1^{(l)}, \text{Vec}_2^{(l)}, \dots, \text{Vec}_C^{(l)}] \\ c_i &= \text{softmax}(v_i^\top \text{Vec}^{(l)} W + b) \\ s_i &= \text{softmax}(\gamma y_i + c_i) \end{aligned} \quad (6)$$

where f^L is the label encoder function to transfer labels $l = [l_1, l_2, \dots, l_C]$ to the label representation matrix $\text{Vec}^{(l)}$, C the number of categories, f^L is implemented by an embedding lookup layer followed by a DNN, c_i the LCV and s_i the SLD. The SLD is then viewed as a soft label that replaces the one-hot vector formed label for model training.

Note that the SLD s_i and the predicted label vector p_i are both probability measures. Here we use the Kullback-

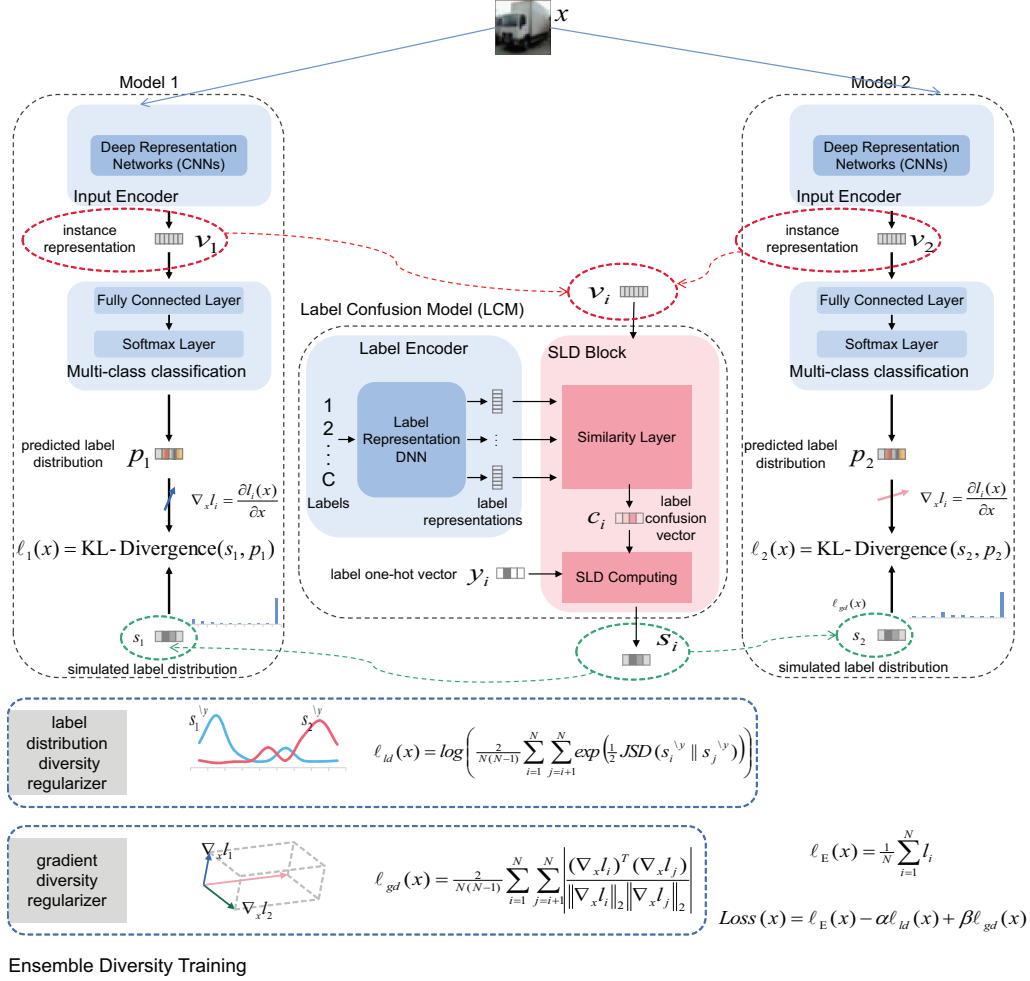


Fig. 2. The proposed CLDL assisted ensemble training method. Here we take an ensemble model that consists of two member models as an example for ease of illustration. Given an image instance x , the label confusion model (LCM) in the middle, which is adapted from [26], is used to generate a soft label s_i for the i th sub-model. Two types of diversity regularizers that are based on the label distribution given the soft labels and the gradient are combined to generate the finally used ensemble diversity regularizer. See the text in Section III for more details.

Leibler (KL) divergence (KL-divergence) [37] to measure their difference:

$$\ell_i(x) = KL\text{-divergence}(s_i, p_i) = \sum_{c=1}^C s_i^c \log \left(\frac{s_i^c}{p_i^c} \right) \quad (7)$$

The LCM is trained by minimizing the above KL divergence, whose value depends on the semantic representation of the image instance v_i and the label s_i learned by the LCM.

A. CLDL based Diversity Regularization

Here we present the diversity regularizer used in our algorithm.

1) *Soft label diversity*: For an input (x, y) in the training dataset, we define the soft label diversity based on the non-maximal value of the SLD of each sub-model. Specifically, let s_i^y be a $(C-1) \times 1$ vector constructed by excluding the maximal value from the SLD corresponding to model $\mathcal{F}_i(x, \theta)$.

Then we use the Jensen-Shannon divergence (JSD) [38] to measure the soft label diversity as follows

$$JSD(s_i^y \| s_j^y) = \frac{1}{2} KL\text{-divergence} \left(s_i^y, \frac{s_i^y + s_j^y}{2} \right) + \frac{1}{2} KL\text{-divergence} \left(s_j^y, \frac{s_i^y + s_j^y}{2} \right) \quad (8)$$

From Eqs. (6) and (8), we see that $JSD(s_i^y \| s_j^y)$ monotonically increases with $JSD(c_i^y \| c_j^y)$. A large JSD indicates a misalignment between the SLDs of the two involved sub-models given the image instance x . Given x and an ensemble of N models, we define the soft label diversity based loss item as follows:

$$\ell_{ld}(x) = \log \left(\frac{2}{N(N-1)} \sum_{i=1}^N \sum_{j=i+1}^N \exp(JSD(s_i^y \| s_j^y)) \right) \quad (9)$$

where $\frac{2}{N(N-1)}$ normalizes the loss over the number of the sub-model pairs in the ensemble.

$$\ell_E(x) = \frac{1}{N} \sum_{i=1}^N \ell_i$$

$$Loss(x) = \ell_E(x) - \alpha \ell_{ld}(x) + \beta \ell_{gd}(x)$$

The more consistent among the SLDs of the sub-models, the more similar among the representations of the image instance x given by the ensemble member models, and vice versa. For an ensemble of N sub-models, we hope that the set of N non-maximal SLDs are maximally misaligned, as this helps to improve the robustness. That says we expect $\ell_{ld}(x)$ to be as big as possible in the ensemble training process.

Note that here we follow [22] to only consider the non-maximal values of the SLDs in defining the diversity measure. In this way, promoting the diversity among the sub-models does not affect the ensemble's prediction accuracy for benign inputs, while it can lower down the attacks' transferability among the sub-models.

2) *Gradient diversity*: Following [21], [25], we also try to promote the sub-models' diversity by minimizing their gradient alignment. By so doing, we can further reduce the overall adversarial transferability among the member models. Given an image instance x and an ensemble of N models, we define the gradient diversity loss item as:

$$\begin{aligned}\ell_{gd}(x) &= \frac{2}{N(N-1)} \sum_{i=1}^N \sum_{j=i+1}^N CS(\nabla_x \ell_i, \nabla_x \ell_j) \\ &= \frac{2}{N(N-1)} \sum_{i=1}^N \sum_{j=i+1}^N \left| \frac{(\nabla_x \ell_i)^T (\nabla_x \ell_j)}{\|\nabla_x \ell_i\|_2 \|\nabla_x \ell_j\|_2} \right| \quad (10)\end{aligned}$$

3) *CLDL based Ensemble Diversity*: Combining the above soft label and gradient diversity loss items, we propose our CLDL based ensemble diversity loss function. For a pair of member models (\mathcal{F} and \mathcal{G}), given an input instance x , this diversity promoting loss function is

$$\ell_{\mathcal{F}, \mathcal{G}, x} = -\alpha \ell_{ld}(x) + \beta \ell_{gd}(x), \quad (11)$$

where $\alpha, \beta \geq 0$ are hyper-parameters that balance the effects of the soft label based and the gradient based diversity loss items.

B. CLDL based Ensemble Model Training

We train our ensemble model by minimizing the training loss defined as follows

$$\text{Loss}(x) = \ell_E(x) + \ell_{\mathcal{F}, \mathcal{G}, x} = \left(\frac{1}{N} \sum_{i=1}^N \ell_i \right) - \alpha \ell_{ld}(x) + \beta \ell_{gd}(x) \quad (12)$$

where $\ell_E(x) = \frac{1}{N} \sum_{i=1}^N \ell_i$ refers to the average of the KL-divergence losses of the member models. See Figure 2 for the definition of the KL loss of the member models.

By minimizing the above loss function, we simultaneously learn the soft labels given by each sub-model, promote the diversity among the sub-models in terms their predicted soft labels and their gradients, and minimize the KL-divergence loss of each sub-model. In the following experiment section, we verify that our loss function design reduces the transferability of adversarial examples and improves the adversarial robustness of the target model against black-box attacks.

We present a pseudo-code of our CLDL assisted ensemble training algorithm in Algorithm 1.

Algorithm 1 CLDL assisted ensemble training for an ensemble of N sub-models

```

1: Input: The  $N$  individual models  $\{\mathcal{F}_i(x, \theta_i)\}_{i \in [N]}$  of the
   ensemble, where  $[N] = \{1, 2, \dots, N\}$ ; The label confusion
   model  $\text{LCM}(v, y, \theta)$ , where  $\theta$  denotes the model
   parameter; a training dataset  $\mathcal{D}_{train} = \{(x_j, y_j)\}_{j \in [M]}$ .
   training epochs  $\mathcal{T}$ 
2: Initialization: Initialize model parameters  $\theta_i$ ,  $\theta$  and the
   learning rates  $\epsilon_i$  and  $\epsilon$ , the indicator set  $\mathcal{I} = [N]$ ,  $\forall i \in [N]$ .

3: for  $t = 1$  to  $\mathcal{T}$  do
4:   for  $iter = 1$  to  $iterations$  do
5:     Sample a mini-batch  $\mathcal{D}_{iter}$  from  $\mathcal{D}_{train}$ 
6:     for  $i$  in  $\mathcal{I}$  do
7:       Obtain the instance representation
          $\{v_j(x_j, \theta_i)\}_{x_j \in \mathcal{D}_{iter}}$  from the outputs of the
         last linear layer of  $\mathcal{F}_i(x_j, \theta_i)$ .
8:       Obtain the predicted label distribution
          $\{p_j(x_j, \theta_i)\}_{x_j \in \mathcal{D}_{iter}}$  from the outputs of soft-max
         layer of  $\mathcal{F}_i(x_j, \theta_i)$ .
9:       Obtain the simulated label distribution
          $\{s_j(x_j, \theta_i)\}_{x_j \in \mathcal{D}_{iter}}$  from  $\text{LCM}(v_j, y_j, \theta)$  by
         Eqn. (6).
10:      Calculate loss  $\ell_i(x_j, \theta_i)_{x_j \in \mathcal{D}_{iter}}$  by Eqn. (7).
11:      Calculate the gradients of the loss  $(\nabla_{x_j} \ell_i)_{x_j \in \mathcal{D}_{iter}}$ .
12:    end for
13:    Calculate the label distribution similarity loss
        $\ell_{ld}(x_j)_{x_j \in \mathcal{D}_{iter}}$  by Eqn. (9)
14:    Calculate the model loss gradient consistency loss
        $\ell_{gd}(x_j)_{x_j \in \mathcal{D}_{iter}}$  by Eqn. (10)
15:    Calculate our LSD regularization loss
        $\ell_{\mathcal{F}, \mathcal{G}}(x_j)_{x_j \in \mathcal{D}_{iter}}$  by Eqn. (11)
16:    Calculate the objective on  $\mathcal{D}_{iter}$ 

       
$$\mathcal{L}_{LSD}^{iter} = \frac{1}{|\mathcal{D}_{iter}|} \sum_{x_j \in \mathcal{D}_{iter}} [\ell_E + \ell_{\mathcal{F}, \mathcal{G}}](x_j).$$


17:    for  $i$  in  $\mathcal{I}$  do
18:       $\theta^i \leftarrow \theta^i - \epsilon_i \nabla_{\theta^i} \mathcal{L}_{LSD}^{iter}|_{\{\theta_i\}_{i \in [N]}}$ 
19:    end for
20:     $\theta \leftarrow \theta - \epsilon \nabla_{\theta} \mathcal{L}_{LSD}^{iter}|_{\{\theta\}}$  for  $\text{LCM}(v, y, \theta)$ .
21:  end for
22: end for
23: return  $\theta^i$  and  $\theta$ ,  $\forall i \in [N]$ .
```

IV. EXPERIMENTS

A. Datasets and Competitor Methods

We do our experiments on the widely-used image datasets MNIST, Fashion-MNIST, and CIFAR-10 [39]. For each dataset, we use its training set to for ensemble model training. We set the hyper-parameter value of our algorithm based on 1,000 test images randomly sampled from the testing set, and use the remaining data in the testing set for performance evaluation.

We compare the performance of our algorithm with several competitor methods, including a baseline method that trains the model ensemble without the use of any defense mechanism,

and four popularly used ensemble training methods, namely the adaptive diversity promoting (ADP) algorithm, the gradient alignment loss (GAL) method, the diversifying vulnerabilities for enhanced robust generation of ensembles (DVERGE) method, and the transferability reduced smooth (TRS) method. Here we use ResNet-20 as the basic model structure of the sub-models. We average the output probabilities given by the soft-max layer of each sub-model to yield the final prediction.

B. Optimizer for Training

We use Adam [40] as the optimizer for ensemble training, set its initial learning rate at 10^{-3} , and the weight decaying parameter at 10^{-4} . For our CLDL based algorithm, we train the ensemble for 200 epochs, multiply the learning rate by 0.1 twice, at the 100th and 150th epochs, respectively. We set the batch size to be 128, and use normalization, random cropping, and flipping based data augmentations for dataset CIFAR-10. We consider two ensemble sizes, 3 and 5, in our experiments. To make a fair comparison, we train ADP, GAL, DVERGE and TRS, under a similar training setup as described above. We use the AdverTorch [41] library for simulating adversarial attacks.

C. White-box Attacks

We consider four basic white-box adversarial attacks, namely FGSM, BIM, MIM, and PGD. Here they are used to simulate the black-box attacks used in our experiments, which are presented in the following subsection. For each type of attack, we consider four different perturbation scales (ϵ) ranging from 0.01 to 0.04. We set the number of attack iterations as 10 and set the step size $\epsilon/5$ for BIM, MIM and PGD. Each experiment is run 5 times independently, and the results are averaged for comparison. We simulate the white-box attacks by treating the whole ensemble, other than one of the individual sub-models, as the target model to be attacked. The performance metric is the classification accuracy, which is defined as the ratio of the number of correctly predicted adversarial instances to the number of all adversarial instances.

D. Black-box Attacks

We consider black-box attack cases, wherein the attacker has no knowledge about the target model to be attacked, including its model architecture and parameters. The attacker design adversarial examples based on several surrogate models. We simulate black-box attacks with our ensemble model as the target, by creating white-box adversarial attacks based on a surrogate ensemble model, which has the same architecture as the true target ensemble, and is trained based on the same dataset using the same training routine.

We train the surrogate ensembles model that consists of 3 or 5 member sub-models by minimizing a standard ensemble cross-entropy loss function. For each type of attacks mentioned in the above subsection, we evaluate the robustness of the involved training methods under the black-box setting with four different perturbation scales (ϵ) 0.01, 0.02, 0.03 and 0.04. We set the number of attack iterations at 10, and the step size

at $\epsilon/5$ for BIM, MIM and PGD based attacks. We apply the Cross Entropy and CW loss functions on each surrogate model to generate adversarial instances.

E. Experimental Results for Black-box Adversarial Attacks

1) *CIFAR-10*: Here we present our experimental results on the dataset CIFAR-10 in Tables I and II. Note that, in all tables shown below, $CLDL_{a,b,c}$ denotes that our CLDL based algorithm's hyper-parameters, namely γ in Eqn.(6), α and β in Eqn.(12) are set at a , b , and c , respectively, and ϵ refers to the perturbation scale of the attack. It is shown that our CLDL based algorithm performs best for almost all of the attacks, compared to the other methods, especially when the perturbation scale is larger.

TABLE I
CLASSIFICATION ACCURACY (%) ON THE CIFAR-10 DATASET FOR FOUR TYPES OF BLACK-BOX ATTACKS. THE ENSEMBLE CONSISTS OF 3 RE NETS-20 MEMBER MODELS. ϵ REFERS TO THE PERTURBATION SCALE FOR THE ATTACK.

CIFAR-10	ϵ	ADP	GAL	DVERGE	TRS	$CLDL_{4,2,4}$	$CLDL_{4,0.5,4}$
BIM	0.01	45.43	92.61	89.66	87.86	92.77	92.77
	0.02	9.74	83.59	75.41	71.17	85.21	83.66
	0.03	2.01	73.02	59.24	53.74	75.76	72.97
	0.04	0.47	62.32	42.27	37.87	66.47	62.38
FGSM	0.01	67.03	93.47	91.20	90.37	93.49	93.47
	0.02	40.58	84.62	78.68	77.59	86.21	85.48
	0.03	26.41	75.93	65.37	64.12	77.94	76.04
	0.04	18.25	66.15	51.40	51.04	69.93	66.95
MIM	0.01	41.65	91.11	87.52	85.39	91.29	91.08
	0.02	7.37	76.92	65.85	61.80	78.98	77.01
	0.03	1.13	59.75	40.35	38.01	63.84	59.89
	0.04	0.30	43.48	19.77	20.24	48.27	43.06
PGD	0.01	46.20	92.41	89.36	88.06	92.18	92.25
	0.02	9.23	83.46	76.08	72.07	84.81	83.68
	0.03	1.55	74.67	61.28	55.12	77.34	75.04
	0.04	0.35	65.46	44.72	39.23	70.64	67.09

TABLE II
CLASSIFICATION ACCURACY (%) ON THE CIFAR-10 DATASET FOR FOUR TYPES OF BLACK-BOX ATTACKS. THE ENSEMBLE CONSISTS OF 5 RE NETS-20 MEMBER MODELS.

CIFAR-10	ϵ	ADP	GAL	DVERGE/5	TRS	$LSD_{4,2,4}$	$LSD_{4,0.5,4}$
BIM	0.01	45.28	92.22	93.32	91.17	93.73	92.89
	0.02	9.50	81.69	85.27	80.15	85.71	84.58
	0.03	1.79	69.68	75.72	67.93	75.93	75.56
	0.04	0.44	57.21	64.59	55.95	65.39	65.8
FGSM	0.01	68.49	93.33	94.22	92.65	94.47	93.54
	0.02	43.02	84.13	86.79	83.30	87.06	85.92
	0.03	27.76	74.15	77.56	72.24	78.79	78.3
	0.04	19.36	64.32	67.10	61.08	69.93	69.68
MIM	0.01	41.77	90.50	91.92	89.53	92.17	91.4
	0.02	7.42	73.95	79.69	73.33	79.33	78.67
	0.03	1.16	55.09	62.87	54.63	63.24	62.93
	0.04	0.25	37.87	44.19	38.76	47.16	46.62
PGD	0.01	46.50	92.22	93.34	91.29	92.92	92.02
	0.02	9.43	81.85	85.60	80.24	85.92	84.45
	0.03	1.54	71.89	77.59	68.25	78.07	76.87
	0.04	0.29	61.60	68.53	55.45	70.05	69.78

We investigate the performance of our algorithm under different hyper-parameter settings in Table III for the above case. As is shown, $CLDL_{4,2,4}$ gives the best results.

TABLE III

CLASSIFICATION ACCURACY (%) GIVEN BY AN ENSEMBLE MODEL CONSISTING OF 3 ReNets-20 MEMBER MODELS TRAINED WITH OUR CLDL BASED ALGORITHM WITH DIFFERENT HYPER-PARAMETER SETTINGS AGAINST BLACK-BOX ATTACKS ON THE CIFAR-10 DATASET.

CIFAR-10	ϵ	CLDL _{4,0,0}	CLDL _{4,1,0}	CLDL _{4,2,0}	CLDL _{4,4,0}	CLDL _{4,1,2}	CLDL _{4,2,2}	CLDL _{4,0.5,4}	CLDL _{4,2,4}
BIM	0.01	89.97	89.66	89.82	89.78	92.76	92.62	92.77	92.77
	0.02	74.01	74.18	74.2	74.42	83.43	82.97	83.66	85.21
	0.03	57.1	56.62	56.78	56.92	73.02	72.64	72.97	75.76
	0.04	40.11	39.63	40.63	40.53	61.8	61.69	62.38	66.47
FGSM	0.01	91.53	91.07	91.01	91.12	93.5	93.2	93.47	93.49
	0.02	78.64	78.63	78.78	78.51	84.79	84.62	85.48	86.21
	0.03	64.83	64.37	65.22	64.37	76.05	76.24	76.04	77.94
	0.04	52.36	51.87	53.11	52.16	66.55	67.42	66.95	69.93
MIM	0.01	87.64	87.18	87.39	87.26	91.22	90.73	91.08	91.29
	0.02	63.63	63.24	63.79	63.86	76.16	76.3	77.01	78.98
	0.03	39.03	38.62	39.29	38.82	58.9	59.25	59.89	63.84
	0.04	20.84	20.29	21.5	21.42	41.79	43.07	43.06	48.27
PGD	0.01	90.24	89.74	89.76	89.75	92.26	92.09	92.25	92.18
	0.02	75.54	75.66	75.48	75.69	83.25	82.81	83.68	84.81
	0.03	60.63	60.03	60.55	60.13	74.53	74.45	75.04	77.34
	0.04	46.97	46.2	46.68	46.41	66.03	65.95	67.09	70.64

2) *MNIST*: In Table IV and Table V, we show classification accuracy (%) results for an ensemble of $N(= 3, 5)$ LeNet-5 member models on the MNIST dataset. In Table VI and Table

TABLE IV

CLASSIFICATION ACCURACY (%) GIVEN BY AN ENSEMBLE MODEL CONSISTING OF 3 LeNet-5 MEMBER MODELS TRAINED WITH OUR CLDL BASED ALGORITHM AGAINST BLACK-BOX ATTACKS ON THE MNIST DATASET.

MNIST	ϵ	ADP	GAL	DVERGE	TRS	CLDL _{3,4,4}	CLDL _{3,2,1}
BIM	0.1	90.18	87.34	90.24	92.5	94.48	94.22
	0.15	60.38	55.61	61.21	76.63	85.64	81.42
	0.2	23.23	28.5	21.17	46.16	65.11	51.59
	0.25	5.32	11.06	2.53	17.42	32.81	22.95
FGSM	0.1	93.29	90.77	93.51	94.55	95.43	95.5
	0.15	79.58	69.94	80.75	86.21	89.82	88.56
	0.2	52.99	47.35	55.98	70.64	78.39	72.73
	0.25	27.38	30.13	27.78	48.1	57.51	46.77
MIM	0.1	90.21	85.82	90.52	92.31	94.25	94.07
	0.15	63.05	53.72	63.67	76.81	85.31	81.56
	0.2	24.69	27.49	23.88	46.83	65.1	51.33
	0.25	5.58	10.64	3.16	16.58	30.44	21.34
PGD	0.1	89.66	84.87	89.82	91.91	93.75	93.84
	0.15	56.83	47.69	57.86	73.01	83.5	78.92
	0.2	19.42	21.69	17.32	39.19	58.94	46.91
	0.25	3.06	6.44	1.05	11.71	24.81	16.65

VII, we show classification accuracy (%) results associated with different hyper-parameter settings.

3) *F-MNIST*: In Table VIII and Table IX, we present results associated with the F-MNIST dataset. In Table X and Table XI, we present results of CLDL associated with different hyper-parameter settings.

4) *hyper-parameter settings*: In this subsection, we investigate the performance of our CLDL based training method against black-box attacks under different hyper-parameter settings.

The value of the hyper-parameter γ determines the extent to which the LCM influences the ensemble training process. For generating the SLD, a larger γ value gives more weight to the original one-hot vector label. We present the results in Tables XII, XIII, and XIV on the datasets CIFAR-10, MNIST, and F-MNIST, respectively. Here an ensemble of 3 member models

TABLE V
ROBUST ACCURACY (%) OF AN ENSEMBLE OF 5 LeNet-5 MODELS AGAINST BLACK-BOX ATTACKS ON THE MNIST DATASET

MNIST	ϵ	ADP	GAL	DVERGE	TRS	CLDL _{3,4,4}	CLDL _{3,2,1}
BIM	0.1	88.43	90.26	89.49	94.01	95.01	93.98
	0.15	53.68	66.19	60.83	82.77	87.18	78.76
	0.2	18.98	34.1	23.04	55.12	68.76	51.46
	0.25	2.21	12.02	4.01	22.2	40.58	25.3
FGSM	0.1	92.23	93.03	92.88	95.41	95.9	95.62
	0.15	75.07	79.74	80.23	88.85	89.86	88.43
	0.2	46.26	58.21	54.71	76.11	76.95	71.07
	0.25	22.41	35.67	29.5	54.6	52.6	44.93
MIM	0.1	89.06	89.62	89.84	93.96	94.68	93.96
	0.15	56.8	66.79	63.58	82.61	85.96	78.68
	0.2	21.1	35.18	26.19	56.63	65.32	50.11
	0.25	3.02	12.37	5.33	22.55	34.31	22.36
PGD	0.1	87.83	88.69	89.11	93.53	94.4	93.49
	0.15	50.51	60.26	57.6	81.19	85.08	74.77
	0.2	15.33	27.47	19.45	50.15	63.35	45.58
	0.25	0.97	6.64	2.19	17.06	31.88	18.38

is used. For CIFAR-10, the model structure is ReNets-20; and the other datasets, the model structure is Lenet-5.

V. CONCLUSION

In this paper, we proposed a CLDL assisted adversarial ensemble training algorithm. In contrast with the existent ensemble training methods which encode the image classes with one-hot vectors, our algorithm can learn and exploit the conditional label dependencies when training the member models. The experimental results show that our algorithm is more robust than SOTA methods against black-box adversarial attacks.

ACKNOWLEDGMENTS

This work was supported by Research Initiation Project (No.2021KB0PI01) and Exploratory Research Project (No.2022RC0AN02) of Zhejiang Lab.

REFERENCES

- [1] K. He, X. Zhang, S. Ren, and J. Sun, "Deep residual learning for image recognition," in *Proceedings of the IEEE conference on computer vision and pattern recognition*, 2016, pp. 770–778.

TABLE VI

CLASSIFICATION ACCURACY (%) OF AN ENSEMBLE OF 3 LeNET-5 MODELS TRAINED WITH OUR CLDL BASED ALGORITHM, UNDER DIFFERENT HYPER-PARAMETER SETTINGS

MNIST	ϵ	$CLDL_{3,0,0}$	$CLDL_{3,1,0}$	$CLDL_{3,2,0}$	$CLDL_{3,4,0}$	$CLDL_{3,1,2}$	$CLDL_{3,1,4}$	$CLDL_{3,2,4}$	$CLDL_{3,4,4}$	$CLDL_{3,2,1}$
BIM	0.1	89.83	89.8	89.45	89.79	93.64	93.55	93.31	94.48	94.22
	0.15	60.81	61.44	61.04	61.56	80.14	80.21	79	85.64	81.42
	0.2	28.04	29.86	30.9	29.28	51.04	53.37	50.56	65.11	51.59
	0.25	9.8	9.74	10.31	9.18	22.87	23.68	20.45	32.81	22.95
FGSM	0.1	92.76	92.85	92.81	92.74	95.07	94.83	94.36	95.43	95.5
	0.15	76.59	76.75	75.58	76.68	87.32	86.61	85.86	89.82	88.56
	0.2	47.47	50.18	50.2	49.68	71.05	69.63	65.53	78.39	72.73
	0.25	26.68	28.08	28.84	27.47	42.38	44.23	36.26	57.51	46.77
MIM	0.1	89.73	89.85	89.51	89.97	93.41	93.09	92.87	94.25	94.07
	0.15	61.41	62.21	61.49	62.19	80.03	79.47	78.6	85.31	81.56
	0.2	28.23	29.97	31.04	29.4	49.38	51.79	48.12	65.1	51.33
	0.25	9.39	9.8	10.05	9.08	18.63	20.66	16.38	30.44	21.34
PGD	0.1	88.99	89.06	88.61	89.3	92.97	92.64	92.53	93.75	93.84
	0.15	57.23	58.2	58	58.52	76.86	77.14	75.13	83.5	78.92
	0.2	23.88	25.75	27.11	25.47	44.3	46.14	41.94	58.94	46.91
	0.25	6.54	6.52	6.62	6	15.54	16.64	11.8	24.81	16.65

TABLE VII

CLASSIFICATION ACCURACY (%) OF AN ENSEMBLE OF 5 LeNET-5 MODELS TRAINED WITH OUR CLDL BASED ALGORITHM, UNDER DIFFERENT HYPER-PARAMETER SETTINGS

MNIST	ϵ	$CLDL_{3,0,0}$	$CLDL_{3,1,0}$	$CLDL_{3,2,0}$	$CLDL_{3,4,0}$	$CLDL_{3,1,2}$	$CLDL_{3,1,4}$	$CLDL_{3,2,4}$	$CLDL_{3,4,4}$	$CLDL_{3,2,1}$
BIM	0.1	89.09	89.08	89.02	89.06	94.63	95.69	95.31	95.01	93.98
	0.15	59.4	60.42	59.7	60.78	82.45	86.9	86.25	87.18	78.76
	0.2	30.63	30.63	30.08	32.04	57.87	65.1	66.16	68.76	51.46
	0.25	11.43	9.2	8.81	9.79	29.54	35.14	37.02	40.58	25.3
FGSM	0.1	92.39	92.52	92.43	92.45	95.71	96.46	96.25	95.9	95.62
	0.15	74.34	75.34	74.43	74.25	88.59	90.72	90.38	89.86	88.43
	0.2	47.05	48.61	48.15	49.83	72.63	76.11	77.44	76.95	71.07
	0.25	27.59	27.19	27.32	28.9	49.24	48.92	54.44	52.6	44.93
MIM	0.1	89.16	89.14	88.98	89.19	94.36	95.64	95.12	94.68	93.96
	0.15	60.14	61.28	60.17	61.4	82.31	86.33	85.3	85.96	78.68
	0.2	29.92	30.29	29.89	31.43	56.53	61.71	62.78	65.32	50.11
	0.25	11.29	9.25	9.08	9.69	26.28	29.34	31.82	34.31	22.36
PGD	0.1	88.16	88.21	88.1	88.22	93.91	95.04	94.81	94.4	93.49
	0.15	56.27	56.87	56.3	57.64	79.47	83.89	83.88	85.08	74.77
	0.2	26.76	26.35	25.96	28.05	51.29	56.57	58.72	63.35	45.58
	0.25	7.81	5.69	5.33	6.05	21.57	24.75	27.48	31.88	18.38

TABLE VIII

CLASSIFICATION ACCURACY (%) OF AN ENSEMBLE OF 3 LeNET-5 MODELS AGAINST BLACK-BOX ATTACKS ON THE F-MNIST DATASET.

F-MNIST	ϵ	ADP	GAL	DVERGE	TRS	$CLDL_{3,2,4}$
BIM	0.08	38.38	54.43	39.42	54.71	54.19
	0.1	28.39	44.37	28.16	44.61	44.99
	0.15	10.55	22.63	10.58	25.06	27.84
	0.2	1.78	7.10	2.69	10.95	13.98
FGSM	0.08	48.25	62.77	52.39	62.83	61.99
	0.1	40.09	54.22	42.80	53.64	53.87
	0.15	23.24	36.09	25.41	37.63	38.49
	0.2	9.82	15.85	13.33	23.45	25.67
MIM	0.08	38.24	52.83	39.58	53.46	52.88
	0.1	28.41	42.44	28.19	43.10	43.41
	0.15	9.17	19.61	9.98	23.01	25.20
	0.2	1.01	3.44	2.33	7.84	9.75
PGD	0.08	37.74	52.34	39.17	52.86	51.65
	0.1	27.75	41.71	28.15	42.38	42.23
	0.15	8.69	18.78	9.67	22.44	24.75
	0.2	1.08	3.52	2.24	8.25	10.91

TABLE IX

CLASSIFICATION ACCURACY (%) OF AN ENSEMBLE OF 5 LeNET-5 MODELS ON THE F-MNIST DATASET

F-MNIST	ϵ	ADP	GAL	DVERGE	TRS	$CLDL_{3,2,4}$
BIM	0.08	38.01	52.62	41.36	60.30	61.37
	0.1	28.57	42.47	29.67	51.10	51.72
	0.15	10.83	23.04	11.15	33.67	35.46
	0.2	2.01	8.86	2.63	20.48	24.58
FGSM	0.08	48.36	62.53	54.13	65.65	67.90
	0.1	39.94	54.14	44.80	58.09	59.78
	0.15	23.00	36.65	27.28	43.66	45.69
	0.2	9.98	19.49	14.44	31.91	32.71
MIM	0.08	38.22	52.16	41.69	58.93	59.18
	0.1	28.65	42.23	30.20	49.41	49.48
	0.15	9.75	20.97	11.27	31.79	33.15
	0.2	1.26	4.94	2.12	17.11	18.71
PGD	0.08	37.76	51.56	41.11	59.06	58.28
	0.1	27.86	41.03	29.50	49.18	47.99
	0.15	9.39	20.45	10.14	31.27	32.97
	0.2	1.39	5.99	1.97	18.00	20.38

- [2] A. Krizhevsky, I. Sutskever, and G. E. Hinton, "Imagenet classification with deep convolutional neural networks," *Advances in neural information processing systems*, vol. 25, 2012.
- [3] O. Russakovsky, J. Deng, H. Su, J. Krause, S. Satheesh, S. Ma, Z. Huang, A. Karpathy, A. Khosla, M. Bernstein *et al.*, "Imagenet large scale visual

- recognition challenge," *International journal of computer vision*, vol. 115, no. 3, pp. 211–252, 2015.
- [4] C. Szegedy, V. Vanhoucke, S. Ioffe, J. Shlens, and Z. Wojna, "Rethinking the inception architecture for computer vision," in *Proceedings of the IEEE conference on computer vision and pattern recognition*, 2016, pp.

TABLE X
CLASSIFICATION ACCURACY (%) OF AN ENSEMBLE OF 3 LeNet-5 MODELS TRAINED WITH OUR CLDL BASED ALGORITHM UNDER DIFFERENT HYPER-PARAMETER SETTINGS ON THE F-MNIST DATASET

F-MNIST	ϵ	CLDL _{3,0,0}	CLDL _{3,1,0}	CLDL _{3,2,0}	CLDL _{3,4,0}	CLDL _{3,1,2}	CLDL _{3,1,4}	CLDL _{3,2,4}	CLDL _{3,4,4}
BIM	0.08	38.48	38.55	38.96	39.09	48.19	53.72	54.19	54.47
	0.1	29.71	29.73	30.22	30.27	39.37	44.04	44.99	44.87
	0.15	11.58	11.36	11.77	11.63	22.11	27.62	27.84	29.23
	0.2	1.30	1.89	2.23	2.08	8.63	14.08	13.98	15.87
FGSM	0.08	49.04	48.40	48.68	48.83	57.36	61.88	61.99	60.90
	0.1	40.45	40.18	40.31	41.13	49.36	53.23	53.87	52.86
	0.15	22.65	23.03	23.11	23.34	32.58	36.78	38.49	37.64
	0.2	10.00	10.53	11.41	11.06	17.21	21.96	25.67	22.31
MIM	0.08	38.75	38.70	39.10	39.53	47.68	52.44	52.88	52.30
	0.1	29.73	29.66	30.22	30.24	38.34	42.93	43.41	43.39
	0.15	9.81	10.09	10.47	10.48	19.29	24.95	25.20	26.42
	0.2	0.82	1.18	1.45	1.30	5.28	9.40	9.75	10.22
PGD	0.08	38.12	38.17	38.68	38.95	46.62	51.76	51.65	52.25
	0.1	29.34	29.50	29.78	29.71	37.25	41.88	42.23	42.63
	0.15	10.14	10.30	10.93	10.87	19.69	24.93	24.75	26.74
	0.2	0.80	1.20	1.58	1.42	6.01	10.63	10.91	12.06

TABLE XI
CLASSIFICATION ACCURACY (%) OF AN ENSEMBLE OF 5 LeNet-5 MODELS TRAINED WITH OUR CLDL BASED ALGORITHM UNDER DIFFERENT HYPER-PARAMETER SETTINGS ON THE F-MNIST DATASET

F-MNIST	ϵ	CLDL _{3,0,0}	CLDL _{3,1,0}	CLDL _{3,2,0}	CLDL _{3,4,0}	CLDL _{3,1,2}	CLDL _{3,1,4}	CLDL _{3,2,4}	CLDL _{3,4,4}
BIM	0.08	40.50	40.32	40.57	40.67	54.94	62.99	61.37	58.89
	0.1	32.13	31.55	31.98	32.15	45.67	53.85	51.72	49.70
	0.15	13.20	13.21	13.28	13.34	30.40	38.63	35.46	34.63
	0.2	2.91	2.55	2.64	2.74	17.57	25.77	24.58	21.60
FGSM	0.08	50.11	50.19	50.21	50.02	62.17	68.85	67.90	65.80
	0.1	42.33	42.31	42.54	42.59	53.84	60.55	59.78	57.30
	0.15	25.86	25.46	25.88	25.81	38.46	45.55	45.69	42.11
	0.2	12.78	12.48	12.53	12.47	24.94	31.14	32.71	27.94
MIM	0.08	40.53	40.49	40.82	40.83	53.14	61.23	59.18	57.10
	0.1	31.95	31.50	31.97	31.93	44.49	52.31	49.48	47.83
	0.15	11.89	11.94	12.16	12.06	27.94	35.00	33.15	31.04
	0.2	1.76	1.67	1.63	1.61	13.49	19.32	18.71	16.10
PGD	0.08	40.29	40.20	40.41	40.27	52.72	60.01	58.28	56.55
	0.1	31.99	31.32	31.75	31.83	43.34	50.95	47.99	47.02
	0.15	11.90	11.97	11.92	11.88	28.22	34.72	32.97	31.24
	0.2	1.96	1.77	1.81	1.76	14.62	19.92	20.38	17.20

2818–2826.

- [5] A. Graves and N. Jaitly, “Towards end-to-end speech recognition with recurrent neural networks,” in *International conference on machine learning*. PMLR, 2014, pp. 1764–1772.
- [6] A. Hannun, C. Case, J. Casper, B. Catanzaro, G. Diamos, E. Elsen, R. Prenger, S. Satheesh, S. Sengupta, A. Coates *et al.*, “Deep speech: Scaling up end-to-end speech recognition,” *arXiv preprint arXiv:1412.5567*, 2014.
- [7] I. Sutskever, O. Vinyals, and Q. V. Le, “Sequence to sequence learning with neural networks,” *Advances in neural information processing systems*, vol. 27, 2014.
- [8] B. Xu, R. Cai, Z. Zhang, X. Yang, Z. Hao, Z. Li, and Z. Liang, “Nadaq: natural language database querying based on deep learning,” *IEEE Access*, vol. 7, pp. 35 012–35 017, 2019.
- [9] I. J. Goodfellow, J. Shlens, and C. Szegedy, “Explaining and harnessing adversarial examples,” *arXiv preprint arXiv:1412.6572*, 2014.
- [10] N. Papernot, P. McDaniel, S. Jha, M. Fredrikson, Z. B. Celik, and A. Swami, “The limitations of deep learning in adversarial settings,” in *2016 IEEE European symposium on security and privacy (EuroS&P)*. IEEE, 2016, pp. 372–387.
- [11] N. Carlini and D. Wagner, “Towards evaluating the robustness of neural networks,” in *2017 IEEE symposium on security and privacy (sp)*. IEEE, 2017, pp. 39–57.
- [12] A. Madry, A. Makelov, L. Schmidt, D. Tsipras, and A. Vladu, “Towards deep learning models resistant to adversarial attacks,” *arXiv preprint arXiv:1706.06083*, 2017.
- [13] C. Xiao, B. Li, J.-Y. Zhu, W. He, M. Liu, and D. Song, “Generating adversarial examples with adversarial networks,” *arXiv preprint arXiv:1801.02610*, 2018.
- [14] C. Xiao, J.-Y. Zhu, B. Li, W. He, M. Liu, and D. Song, “Spatially transformed adversarial examples,” *arXiv preprint arXiv:1801.02612*, 2018.
- [15] N. Papernot, P. McDaniel, and I. Goodfellow, “Transferability in machine learning: from phenomena to black-box attacks using adversarial samples,” *arXiv preprint arXiv:1605.07277*, 2016.
- [16] Y. Liu, X. Chen, C. Liu, and D. Song, “Delving into transferable adversarial examples and black-box attacks,” *arXiv preprint arXiv:1611.02770*, 2016.
- [17] N. Inkawhich, K. J. Liang, L. Carin, and Y. Chen, “Transferable perturbations of deep feature distributions,” *arXiv preprint arXiv:2004.12519*, 2020.
- [18] A. Ilyas, S. Santurkar, D. Tsipras, L. Engstrom, B. Tran, and A. Madry, “Adversarial examples are not bugs, they are features,” *Advances in neural information processing systems*, vol. 32, 2019.
- [19] A. I. Maqueda, A. Loquercio, G. Gallego, N. García, and D. Scaramuzza, “Event-based vision meets deep learning on steering prediction for self-driving cars,” in *Proceedings of the IEEE Conference on Computer Vision and Pattern Recognition*, 2018, pp. 5419–5427.
- [20] M. Bojarski, D. Del Testa, D. Dworakowski, B. Firner, B. Flepp, P. Goyal, L. D. Jackel, M. Monfort, U. Muller, J. Zhang *et al.*, “End to end learning for self-driving cars,” *arXiv preprint arXiv:1604.07316*, 2016.
- [21] S. Kariyappa and M. K. Qureshi, “Improving adversarial robustness of ensembles with diversity training,” *arXiv preprint arXiv:1901.09981*, 2019.
- [22] T. Pang, K. Xu, C. Du, N. Chen, and J. Zhu, “Improving adversarial robustness via promoting ensemble diversity,” in *International Conference on Machine Learning*. PMLR, 2019, pp. 4970–4979.
- [23] S. Sen, B. Ravindran, and A. Raghunathan, “EMPIR: Ensembles of mixed precision deep networks for increased robustness against adver-

TABLE XII

CLASSIFICATION ACCURACY (%) OF AN ENSEMBLE OF 3 LeNET-5 MODELS TRAINED WITH CLDL UNDER DIFFERENT HYPER-PARAMETER SETTINGS AGAINST BLACK-BOX ATTACKS ON THE CIFAR-10 DATASET

		Blackbox						
CIFAR-10	γ	ϵ	α	β				
				0	0.5	1	2	4
BIM		0.03	0.5	53.72	64.07	66.31	68.19	71.6
			1	52.81	65.36	65.8	70.82	72.63
			2	55.25	63.97	66.38	70.41	75.33
			4	55.33	65.03	67.03	70.92	72.19
		0.04	0.5	38.51	48.16	53.46	56.97	60.94
			1	36.69	50.98	53.16	59.45	62.92
			2	38.14	50.22	52.22	57.42	65.68
			4	38.37	50.93	54.26	60.57	63.47
FGSM		0.03	0.5	62.68	69.91	70.19	72.55	74.76
			1	60.71	70.81	72	73.99	76.77
			2	61.32	69	71.78	75	78.51
			4	63.37	69.95	72.16	75.05	74.92
		0.04	0.5	48.98	57.68	59.94	62.09	64.64
			1	49.13	59.69	60.89	64.15	69.36
			2	49.62	59.5	61.19	63.43	68.97
			4	50.22	59.13	61.79	66.23	67.72
MIM		0.03	0.5	36.68	46.86	52.05	53.81	59.85
			1	37.34	48.37	50.98	57.05	61.29
			2	37.27	48.25	50.81	56.55	65.13
			4	36.74	48.52	52.62	58.39	62.6
		0.04	0.5	20.5	31.6	34.99	36.71	42.76
			1	19.16	30.39	32.35	41.2	44.82
			2	20.15	30.02	33.08	41.27	47.04
			4	20.43	32.35	34.28	40.41	46.67
PGD		0.03	0.5	56.85	67.86	68.03	70.15	73.12
			1	56.71	68.08	70.04	72.79	74.15
			2	57.2	67.25	68.32	71.83	75.77
			4	58.04	67.98	69.43	72.55	73.72
		0.04	0.5	45.2	55.63	58.32	61.11	66.16
			1	44.48	57.3	59.04	64.04	68.48
			2	44.53	56.11	58.05	62.99	68.53
			4	45.43	55.96	59.39	64.6	68.38

TABLE XIII

CLASSIFICATION ACCURACY (%) OF AN ENSEMBLE OF 3 LeNET-5 MODELS TRAINED WITH CLDL UNDER DIFFERENT HYPER-PARAMETER SETTINGS AGAINST BLACK-BOX ATTACKS ON THE MNIST DATASET

		Blackbox						
MNIST	γ	ϵ	α	β				
				0	0.5	1	2	4
BIM		0.2	0.5	28.83	39.76	43.09	43.72	56.87
			1	30.47	43.03	43.03	51.62	54.05
			2	31.18	45.56	52.73	45.15	51.52
			4	29.74	45.77	44.49	48.78	65.25
		0.25	0.5	9.38	12.21	17.36	16.5	24.65
			1	9.89	15.45	16.26	24.44	24.9
			2	10.7	18.45	23.64	19.19	19.7
			4	9.88	20.16	20.22	18.86	32.63
FGSM		0.2	0.5	48.69	61.76	57.82	67.81	74.04
			1	50.15	62.53	60.1	72.32	71.26
			2	50.15	67.74	74.04	66.57	65.56
			4	49.4	62	66.13	64.81	80.2
		0.25	0.5	26.92	33.5	31.69	37.96	47.58
			1	26.54	35.86	31.31	40.51	43.72
			2	28.56	38.41	46.97	40.1	35.86
			4	26.92	38.71	40.34	43.1	57.58
MIM		0.2	0.5	28.93	38.55	41.17	42.61	53.84
			1	29.87	41.72	41.31	48.79	52.43
			2	31.38	43.95	51.41	44.14	48.38
			4	30.24	43.95	43.17	49.09	64.75
		0.25	0.5	8.57	10.8	14.73	13.36	23.03
			1	9.69	14.44	12.83	18.59	20.34
			2	10.09	16.63	22.73	16.67	15.66
			4	9.07	17.74	18.2	19.47	31.41
PGD		0.2	0.5	24.09	34.11	38.14	36.74	46.46
			1	26.34	35.96	36.97	44.85	47.27
			2	26.94	39.31	48.08	39.49	42.42
			4	25.1	40.12	40.04	42.6	60.4
		0.25	0.5	5.14	6.86	10.39	8.6	15.45
			1	5.95	8.79	10.3	16.06	16.8
			2	6.76	12.5	16.67	12.22	11.92
			4	6.25	14.72	13.45	13.18	24.85

TABLE XIV

CLASSIFICATION ACCURACY (%) OF AN ENSEMBLE OF 3 LeNET-5 MODELS TRAINED WITH CLDL UNDER DIFFERENT HYPER-PARAMETER SETTINGS AGAINST BLACK-BOX ATTACKS ON THE F-MNIST DATASET

		Blackbox						
F-MNIST	γ	ϵ	α	β				
				0	0.5	1	2	4
BIM		0.08	0.5	37.83	46.64	46.35	45.68	50.21
			1	37.12	46.81	46.21	48.12	52.56
			2	38.26	47.13	46.37	48.28	54.03
			4	37.94	45.69	46.74	47.86	51.4
		0.1	0.5	28.91	37.99	37.23	36.71	40.24
			1	27.47	38.4	36.93	36.87	42.52
			2	29.44	37.66	37.71	37.88	43.61
			4	29.65	36.53	37.43	36.11	43.33
FGSM		0.08	0.5	49.52	56.88	56.33	54.86	58.15
			1	48.67	56.06	55.82	56.48	61.32
			2	48.57	55.85	56.52	56.97	62.41
			4	48.78	56.02	57.65	55.66	60.11
		0.1	0.5	39.32	49.52	48.39	47.6	49.79
			1	39.13	48.4	48.67	50.16	52.56
			2	39.74	49.04	49.68	49.79	54.78
			4	40.17	48.14	49.3	49.04	51.94
MIM		0.08	0.5	37.94	46.53	45.71	45.46	49.57
			1	37.01	46.38	46	46.52	51.39
			2	38.58	46.28	46.26	47.85	51.99
			4	38.04	45.15	45.67	46.58	50.43
		0.1	0.5	29.44	37.89	36.59	35.86	37.88
			1	28.42	37.34	36.07	36.33	41.45
			2	29.54	37.23	36.65	36.37	42.75
			4	29.65	37.38	36.26	35.26	42.8
PGD		0.08	0.5	37.41	45.46	44.64	44.18	47.21
			1	36.59	45.32	45.04	46.09	50.43
			2	37.62	46.38	44.55	45.92	51.45
			4	37.62	44.62	45.35	44.98	49.57
		0.1	0.5	28.27	37.35	35.84	34.69	37.12
			1	27.57	36.6	34.9	35.26	39.64
			2	28.59	36.38	36	35.73	41.46
			4	28.48	35.46	35.61	34.19	40.97

serial attacks,” in *International Conference on Learning Representation (ICLR)*, 2020, pp. 1–12.

- [24] S. Zhang, M. Liu, and J. Yan, “The diversified ensemble neural network,” *Advances in Neural Information Processing Systems*, vol. 33, pp. 16001–16011, 2020.
- [25] Z. Yang, L. Li, X. Xu, S. Zuo, Q. Chen, P. Zhou, B. Rubinstein, C. Zhang, and B. Li, “Trs: Transferability reduced ensemble via promoting gradient diversity and model smoothness,” *Advances in Neural Information Processing Systems*, vol. 34, 2021.
- [26] B. Guo, S. Han, X. Han, H. Huang, and T. Lu, “Label confusion learning to enhance text classification models,” in *Proceedings of the AAAI Conference on Artificial Intelligence*, 2020.
- [27] K. Ren, T. Zheng, Z. Qin, and X. Liu, “Adversarial attacks and defenses in deep learning,” *Engineering*, vol. 6, no. 3, pp. 346–360, 2020.
- [28] X. Yuan, P. He, Q. Zhu, and X. Li, “Adversarial examples: Attacks and defenses for deep learning,” *IEEE Transactions on Neural Networks and Learning Systems*, vol. 30, no. 9, pp. 2805–2824, 2019.
- [29] H. Xu, Y. Ma, H.-C. Liu, D. Deb, H. Liu, J.-L. Tang, and A. K. Jain, “Adversarial attacks and defenses in images, graphs and text: A review,” *International Journal of Automation and Computing*, vol. 17, no. 2, pp. 151–178, 2020.
- [30] A. Kurakin, I. Goodfellow, S. Bengio *et al.*, “Adversarial examples in the physical world,” 2016.
- [31] Y. Dong, F. Liao, T. Pang, H. Su, J. Zhu, X. Hu, and J. Li, “Boosting adversarial attacks with momentum,” in *Proceedings of the IEEE conference on computer vision and pattern recognition*, 2018, pp. 9185–9193.
- [32] Z. Akata, F. Perronnin, Z. Harchaoui, and C. Schmid, “Label-embedding for image classification,” *IEEE Transactions on Pattern Analysis and Machine Intelligence*, vol. 38, no. 7, pp. 1425–1438, 2016.
- [33] R. Muller, S. Kornblith, and G. E. Hinton, “When does label smoothing help,” *arXiv: Learning*, 2019.
- [34] X. Zhang, Q.-W. Zhang, Z. Yan, R. Liu, and Y. Cao, “Enhancing label correlation feedback in multi-label text classification via multi-task learning,” *arXiv preprint arXiv:2106.03103*, 2021.
- [35] C. Fu, H. Chen, N. Ruan, and W. Jia, “Label smoothing and adversarial robustness,” *arXiv preprint arXiv:2009.08233*, 2020.
- [36] Y. Wang, Y. Zheng, Y. Jiang, and M. Huang, “Diversifying dialog gen-

- eration via adaptive label smoothing,” *arXiv preprint arXiv:2105.14556*, 2021.
- [37] S. Kullback and R. A. Leibler, “On information and sufficiency,” *Annals of Mathematical Statistics*, vol. 22, no. 1, pp. 79–86, 1951.
 - [38] M. Menéndez, J. A. Pardo, L. Pardo, and M. C. Pardo, “The jensen-shannon divergence,” *Journal of the Franklin Institute*, vol. 334, no. 2, pp. 307–318, 1997.
 - [39] A. Krizhevsky and G. Hinton, “Learning multiple layers of features from tiny images,” *Technical Report, Department of Computer Science, University of Toronto*, 2009.
 - [40] D. P. Kingma and J. Ba, “Adam: A method for stochastic optimization,” *arXiv preprint arXiv:1412.6980*, 2014.
 - [41] G. W. Ding, L. Wang, and X. Jin, “Advertorch v0. 1: An adversarial robustness toolbox based on pytorch,” *arXiv preprint arXiv:1902.07623*, 2019.